Analysis of hydraulic risk territories: comparison between LIDAR and other different techniques for 3D modeling

VINCENZO BARRILE (*), GIULIANA BILOTTA (**), ANTONINO FOTIA (*)
* DICEAM - Faculty of Engineering
"Mediterranea" University of Reggio Calabria
Via Graziella Feo di Vito 89100 Reggio Calabria, Tel +39 0965 875301
** Ph.D. NT&ITA – Dept. of Planning - University IUAV of Venice
Santa Croce 191, Tolentini 30135 Venice
ITALY
vincenzo.barrile@unirc.it, giuliana.bilotta@iuav.it,antonino.fotia@unirc.it,.

Abstract: - Aim of this paper is investigation of a possible use of the technique of LIDAR topographic survey for updating existing hydraulic models for the calculation of Hydraulic head for risk areas. Specifically, this study intends to assess the benefits to be gained from new methods of LIDAR detection comparing calculations and simulations of updated models with those obtained from existing models, highlighting the critical issues of the use made for hydraulic analysis. We also carried out a comparison on the accuracy obtainable from DEM generated with different methods of acquisition and processing.

Key-Words: Lidar – Hydraulic models– Updating hydraulic models– Hydraulic analysis – DEM

1 Introduction

Among possible uses of the technique of topographic survey, there is the updating of existing hydraulic models for the calculation of Hydraulic head for risk areas.

Generally at the competent institutions are hydraulic models developed on the basis of maps for the reconstruction of the geometry of the waterway and land survey classics, to the party in riverbed with sections made every 100/200 m.

A hydraulic model is a logical-mathematical abstraction for studying behavior and evolution of the flow of waterways that allows, through appropriate software, to simulate the propagation of the flood wave along the hydraulic lattice and then determine the height that the water level reaches in the various sections highlighting possible critical of the lattice itself.

In order to make a productive comparison between models obtained by techniques of classical survey and those by LIDAR, the first step of the study involved the modeling with the same software available; therefore, on the basis ofthe existing topographic survey, we made new hydraulic models, calibrated on the basis of transit times recorded in some major flood events.

Fig.1: Detail and Orthophoto of stream segment.

2 Application of Lidar survey for updating hydraulic model

The LIDAR (Light Detection And Ranging) system is a technique for aerial surveying with the use of an integrated active sensor laser, and GPS and INS. It allows determining position and orientation, the reconstruction of digital models of the surveyed surfaces (DSM) rapidly, with high density of collected points and with planimetric and altimetrical accuracy in the order of 10-30 cm.

The survey through LIDAR occurs with anairplane, or helicopter, on which there is a scanning laser system that integrates four main units:a laser-scanner composed by a laser sensor which emits electric pulses, an acquisition unit, an apparatus for positioning satellite (GPS) and an inertial navigation system (INS), to define position (x, y) and orientation in every moment. On the ground it is installed a network GPS positioning differential.

The waterways are subject to continuous morphological changes both in river morphology that in section because of erosion, transport, sedimentation with the need of a regular update for hydraulic tests.

The advantages of using the LIDAR over the execution speed are especially those of the opportunity to obtain a more precise and detailed real-section; the use of topographic classical surveys involves in effect, for reconstructing the geometry of the intermediate portions between the topographic sections, the use of interpolation with a consequent approximate description.

The technology arose in the late 70s in the United States, and it is diffusely used and for various uses such as for coastal monitoring and risk analysis of sea erosion, the hydraulic risk assessments. It is used also for surveys of environmental (e.g. the search for contaminated sites), forest management (for measurement of critical parameters such as density, height of the stems etc.), linear important infrastructures (power lines, pipelines), and monitoring of mining activities.

The filtering is the first of the phase of the post-processing of raw data that it would otherwise be unusable. To proceed to the identification, for instance, of the super structures present in an area detected, it is necessary to proceed to the separation of the points that belong to the ground than those relating to the objects that are above it [1],[2].

We generally refer to this operation with the term "filtration", that is thus the operation of automatic deletion of points not belonging to the ground surface, and the identification and removal of corresponding points to:

- Approximate errors of measurement (outlier): for some instrumental error can roughly be recognized as "too low" or "too high";
- Buildings, vegetation, "small objects" (cars, enclosing walls).

In operational terms, the filtering is that operation that allows the creation of DTM, that is the surface in irregular triangular meshes (triangulated irregular network, TIN) Delaunay or regular grid passing through points only "land", that differs from the DSM, passing instead through "all" the points raised[3],[4].

Exist in the literature numerous filtering algorithms that can be grouped in two main categories: one based on a mathematical approach to primarily geometrical-local, the other on analytical models statistical-global.

In the present discussion, the step oftreatment and processing of data from the LIDAR survey we used two filtering algorithms. The first is characterized by a global statistical approach to solving the problem; it uses a particular regressive spatial model said SAR Simultaneous Autoregressive.

This approach allows the simultaneous autoregressive estimation both of the trend of the ground surface both of the possible degree of spatial interaction between the laser measurements.

The specificity of the SAR models for estimating deterministic parameters of a surface is given by the fact that these take into account, simultaneously, the topographical relation existing between the points acquired with the laser through the definition of an adjacency matrix W of the various pairs of points. If the generic pair i-j is considered relative to two points topographically next and morphologically related, to its term w_{ij} of the adjacency matrix W will be assigned a weight greater than zero, typically equal to 1. If not, that is, when the two considered points have not topographical relation, this coefficient w_{ij} is set equal to zero [5].

The adjacency matrix W is also multiplied by a coefficient ρ, common to all the points, which expresses the measure of spatial interaction of the observations. Assign a zero value to this coefficient ρ, means to ignore the contribution to the regression model from the adjacency matrix

and then cancel the dependence of the topographical sampled points.

The basic equation of the model is:

$$z - A\vartheta = \left(I - \rho W\right)^{-1} e \quad (1)$$

where:

- *z*vector [*n*x1] of$H_i$altitudes of*n* laser points;
- *A*matrix [*nxr*] of polynomial coefficients, function of the coordinates E_i, N_i, depicting the deterministic trend of the surface;
- $\theta = \left[\theta_0 \theta_1 \ldots \theta_{r-1}\right]^T$ vector [*r*x1] containing the r unknown parameters of the polynomial;
- *I*identitymatrix [*nxn*];
- ρ coefficientof spatialaverage interaction between the laser measurements;
- *W* matrix [*nxn*] of adjacency space between the various pairs of laser points;
- ε vector [*n*x1] of residuals.

It is called outlier observation that is significantly different from observations near to it; this characteristic, in the context of spatial data, is manifested by the move away of a generic measure a trend surface deterministic.

For the model is correctly specified that it is required that (I - ρW) is not unique that is reversible.

To this end they pose of the conditions of W and ρ (namely on the eigenvalues of W). It is assumed that data are distributed as a multivariate Gaussian distribution.

Accordingly, the search Forward Block Search of outliers is via the standardized vector of residuals, whichis obtained from:

$$\hat{\mathbf{e}} = \hat{\sigma}^{-1}\left(\mathbf{I} - \hat{\rho}\mathbf{W}\right)\left(\mathbf{z} - \mathbf{A}\hat{\boldsymbol{\theta}}\right) \quad (2)$$

where $\hat{\theta}$, $\hat{\sigma}$, $\hat{\rho}$, are referring to the maximum likelihood estimation of unknown quantities obtained by maximizing the likelihood function:

$$l\left(\boldsymbol{\theta};\sigma^2;\rho\right) = \left(2\pi\sigma^2\right)^{-n/2}\left|\mathbf{I} - \rho\mathbf{W}\right|\exp\left\{-\frac{1}{2\sigma^2}(\mathbf{z} - \mathbf{A}\boldsymbol{\theta})^{\mathrm{T}}\boldsymbol{\Sigma}(\mathbf{z} - \mathbf{A}\boldsymbol{\theta})\right\} \quad (3)$$

Where$\Sigma$is an appropriate weight matrix, symmetric, positive definite and given by:

$$\boldsymbol{\Sigma} = \left(\mathbf{I} - \rho\mathbf{W}\right)^{\mathrm{T}}\left(\mathbf{I} - \rho\mathbf{W}\right) \quad (4)$$

The errors are not independent from the observations, unlike what happens in the time series; also, this implies that the least squares estimators are not necessarily consistent.

The trend of the ground surface obtained by applying the model equation is likely if, and only if, the points considered in the process of estimating autoregressive belong to the land itself; it is a not satisfied condition when you consider all the laser points acquired. It is then necessary to identify with certainty a subset of points that definitely belong to the soil, said subset outlier-free, by which correctly to estimate the trend.

The class of algorithms called Block Forward Search (BFS) is a particularly innovative and effective analysis and robust estimation and joint trend and parameters of autocorrelation in spatial models.

The second algorithm is a multi-scale based on the concept of multi-fractals technics.

This approach wants to simulate the behavior of the human being and in particular the ability to identify properties that characterize the objects and from these to extract information.

The automated procedure is using a typical function of the multi-fractal analysis applicable to one-dimensional signals:

$$< \left|f(x) - f(x+s)\right|^q > = As^{\tau_q},\ s = s_i, i = 1,2....,\max(i) \quad (5)$$

Where*f(x)* is the function of interest, *s* is the scale, *q* is the power used to produce different exponents multi-fractals τ_q, $< \left|f(x) - f(x+s)\right|^q >$ is the average of $\left|f(x) - f(x+s)\right|^q$ in a given area.

Applying a log function, we have:

$$\log < \left|f(x) - f(x+s)\right|^q > = \tau_q \log(s) + \log(A) \quad (6)$$

Finally, we can calculate the multi-fractals exponents as the slope of $< \left|f(x) - f(x+s)\right|^q >$.

This approach appears to be effective in correctly identifying artificial objects (eg buildings) both large and small; instead, the vegetation can be effectively removed using other methods such as the approach of maximum slope and small median filters[6],[7],[8].

In order to make the application more suited to the processing of LIDAR data, the function:

$$\left| f(x) - f(x+s) \right| \quad (7)$$

is replaced with the

$$f(x) - \min_{\xi \in \aleph_s} f(\xi) \quad (8)$$

with :

$$\aleph_s : \left\{ \xi \in (x - \frac{s-1}{2}, x + \frac{s-1}{2}) \right\} \quad (9)$$

The two functions are similar because both represent the difference in two different areas in a given area defined by the scale *s* but the second is computationally simpler and therefore represents a great advantage since it is applied to Lidar data, which, as known, provide for processing a huge amount of data. So the procedure for the analysis multi-fractals for two dimensions becomes:

$$< \left(f(x,y) - \min_{(\xi,\zeta) \in \aleph_s} f(\xi,\zeta) \right)^q > = As^{\tau_q(s)} \quad (10)$$

With

$$\aleph_s : \left\{ \begin{matrix} \xi \in (x - \frac{s-1}{2}, x + \frac{s-1}{2}) \\ \zeta \in (y - \frac{s-1}{2}, y + \frac{s-1}{2}) \end{matrix} \right\} \quad (11)$$

Applying the log function, we obtained:

$$\log < \left(f(x,y) - \min_{(\xi,\zeta) \in \aleph_s} f(\xi,\zeta) \right)^q > = \tau_q(s) \log(s) + \log(A) \quad (12)$$

Deriving we have

(13)

The function is then:

$$F_q = \max_s \left(\tau_q(s) \right) \quad (14)$$

The function can then be calculated as the greatest exponent of multi-fractal than the scale factor *s* eliminating the dependence on scale.

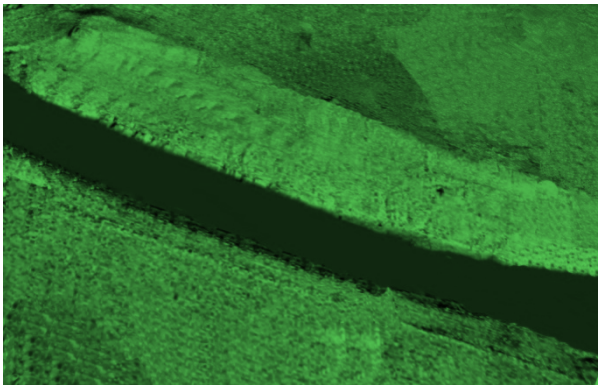

Fig.2: Filtered Lidar image.

After the step of filtering, it is clear that a comparison between Lidar survey and that obtained from topographic sections immediately springs errors both in the engraved riverbed for the very limits of LIDAR in the submerged party, and at the walls of the engraved riverbed, probably for the presence of dense vegetation (Fig.3).

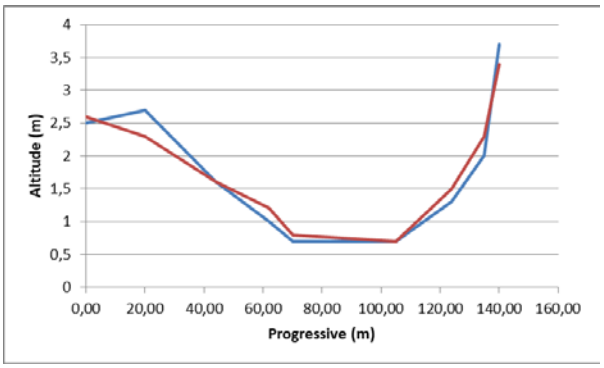

Fig.3: Graphical representation of example of one sections, with overlap between the traditional topographic survey (in blue) and LIDAR (magenta).

Topographic attributes frequently used in hydrologic analyses are derived directly from DEMs [9].

These errors can be reduced in developing phase with an appropriate setting of the parameters in the algorithms for filtering, or in acquiring phase by integrating appropriate LIDAR survey with GPS point measurements on which to calibrate the DEM.

To overcome the problem, it was decided to use the information of the original topographic surveys and sections interpolated relative to the engraved riverbed while, on the geometry of the

river, at the bends, more subject to morphological changes, and at the banks, the information was integrated with GPS point measurements.

The comparison between the model updated with the LIDAR data and that resulting from traditional survey was made by comparing the shape of the hydrograph design flood [10].

It is substantially apparent that the hydrograph shapes are substantially similar, the differences are noted with an increase with the LIDAR survey that in the peak becomes the order of 350m^3/s (Fig.4).

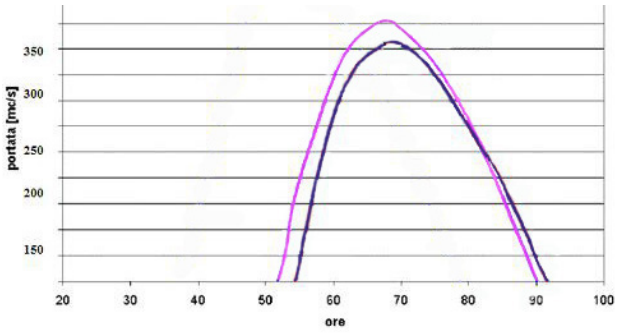

Fig.4: Comparing the flood hydrograph propagated with hydraulic models before and after the upgrade with the use of LIDAR (in magenta).

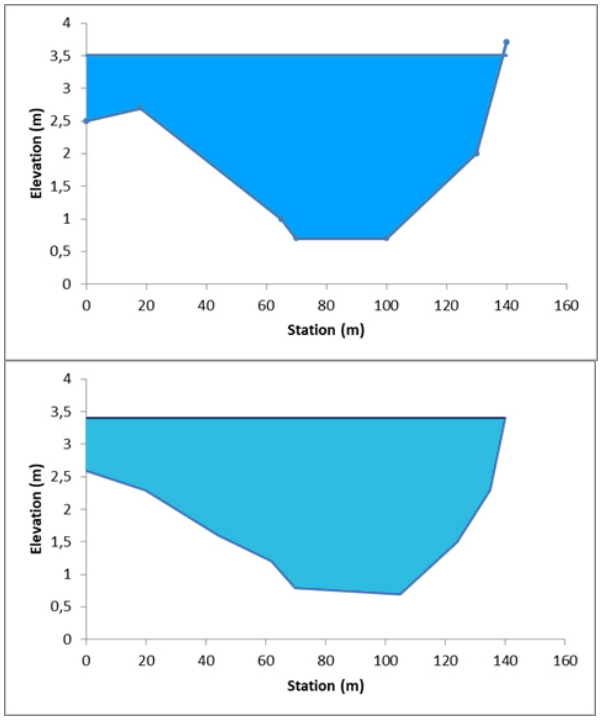

Fig.5: Graphical representation of the maximum levels reached by the flood before and after updating with the use of LIDAR.

Noticeable differences between the two models, however, denote taking the levels where maximum flood, with the LIDAR survey was also possible to consider the riverside areas not present in sections of surveying with classical techniques.

3 Comparison DEMs

We carried out further experimentationsin terms of hydraulic modelling for the comparison of different methods for the construction of DEMs. In particular, we built four DEM including one by classic surveying, another from UAV [11],[12]. [13],[14],[15], another from LIDAR [16],[17]. [18] and another from free mapping with remotely sensed data (SAR), and then we carried out a simulation of hydraulic modeling with HEC-RAS[19],[20].They were validated with reference elevation data. The height precision or quality of each DEM is given by:

$$V_{DEM} = \sqrt{\frac{\sum_{i=1}^{n}\left(E_{R_i} - E_{DEM_i}\right)^2}{n}} \quad (15)$$

In this study, all DEM data are relative to the flood zone. In this area are distributed in situ reference elevation data and this data has been selected from the national geodesy network.

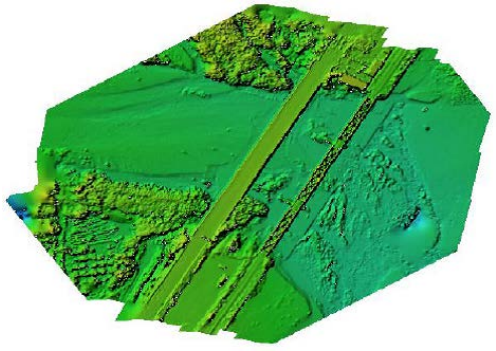

Fig.6: Detail of the Digital model restituted by UAV.

DEM precision according to Eq. (15) is as follows:

- V_{DEM}(Lidar): 0.22 m
- V_{DEM}(contours): 0.30 m
- V_{DEM}(SAR): 0.62 m
- V_{DEM}(UAV): 0.35 m

The LidarDEM gives the best performance with a precision in height of 0.22 m.

However, Lidar has two important limitations. The first is that it provides only discrete surface

height samples and not a continuous coverage. The second is that its availability is really very limited by economic constraints [21].

The performance of the topographic DEM with a height precision of only 0.30m is inadequate. It is connected to the fact that there is not enough variation in height of the area of interest. The effect produced is that there are regions in the resulting DEM with a very poor interpolated estimation of elevation.

The model generated by UAV, compared where possible, presents an even smaller precision than the topographic Dem, and it is also inadequate; we must emphasize, in fact, that the points on which it was possible to make the comparison between DEM, are for the most part within the riverbed.

The SAR DEM has the lowest precision and also the maximum error values and highest variations. The SAR DEM is applicable to large, uniform floodplains to infer advantage hydraulic and hydrologic information thank to its overall height with accuracy of about 0.62m.

Fig.6 shows the graph with the relative performance of different DEMs used.

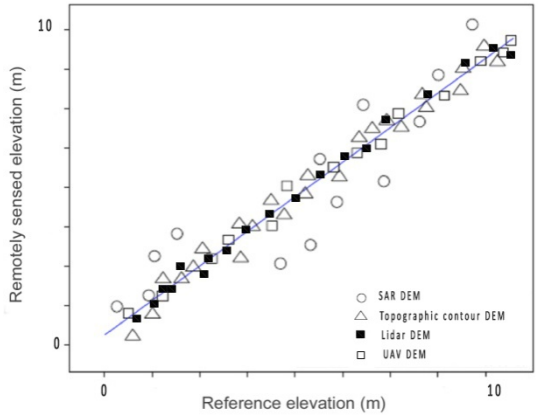

Fig.7: Differences between the various techniques DEM.

With the DEM is possible define the remotely sensed water stages, In Fig. 7 are evident the effects of the data uncertainties inherent in the SAR DEM on remotely sensed water stages. It is clear that there are several zones of flow incoherence, meaning that SAR derived water stages exhibit a lot of incoherent 'jumps' in the direction of the flow, far more than the other two data sets. The results of the erroneous water stages are shown in Figg.8,9,10,11,12.

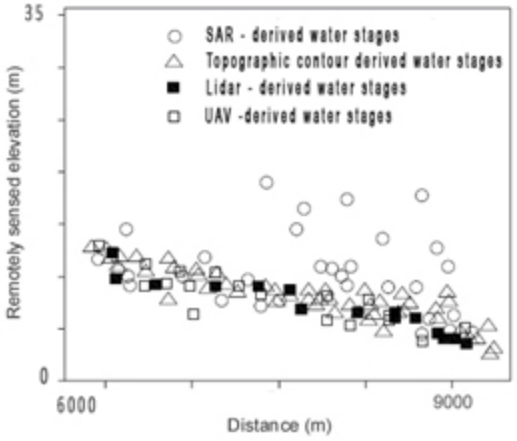

Fig.8. Remotely sensed water stages.

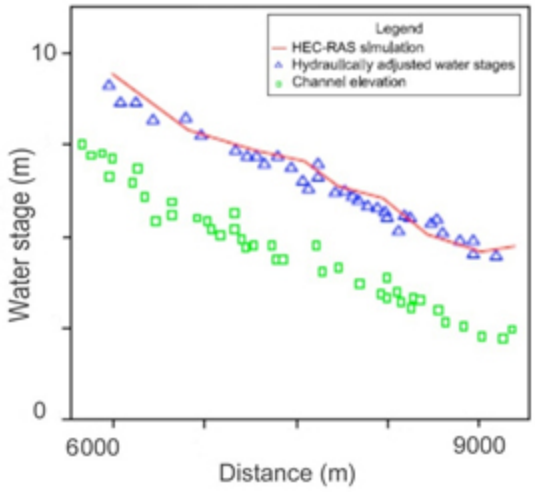

Fig.9: Lidar water stages compared to that simulated by the HEC-RAS model.

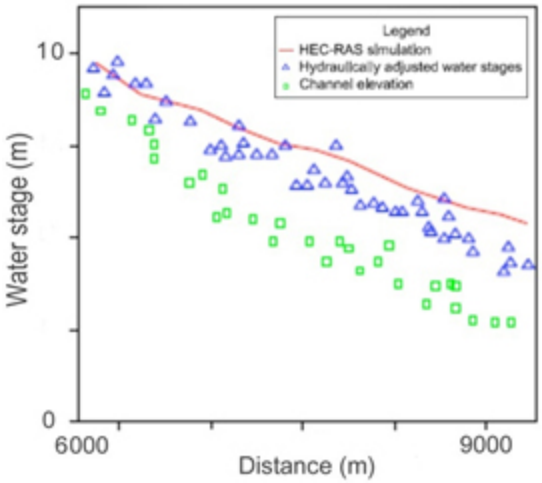

Fig.10: Topographic contours water stages compared to that simulated by the HEC-RAS model.

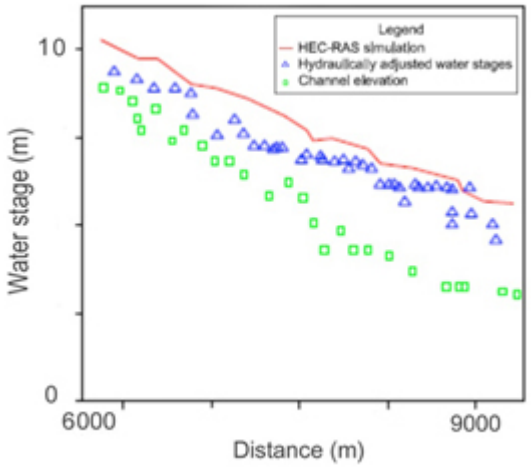

Fig.11: SAR water stages compared to that simulated by the HEC-RAS model.

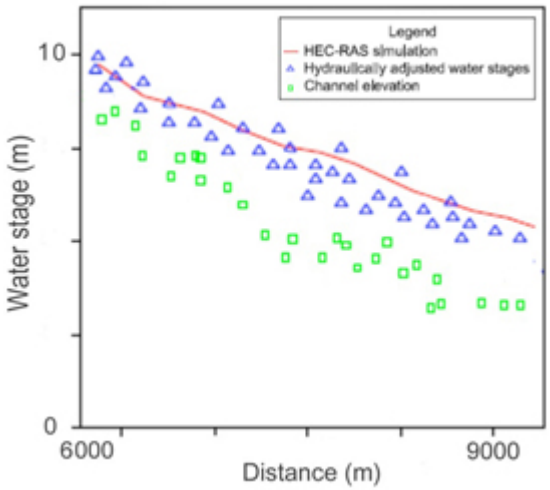

Fig.12: UAV water stages compared to that simulated by the HEC-RAS model.

The Lidar provided the best results. Topographic contours DEM, as well as the DEM obtained by UAV, did not perform as well as expected, as there was insufficient variation in height within the investigated flood-prone area for the generation of a reliable DEM [22].

The SAR is an essential source for initial flood information extraction. It is applied in topographic uniform flood plains, which exhibit a gently sloping river gradient.

4 Conclusions

The application of the detailed topographic elevation with LIDAR technique to one dimensional hydraulic model HEC-RAS, for the case study, has underlined how, with relative ease, you can revise the geometric information in a significant section of the flow.

HEC-RAS is a computer program that models the hydraulics of water flow through natural rivers and other channels. The software allows to perform a modeling in various motion with one-dimensional scheme (1D) combined also withan almost two-dimensional schema and/or a pure two-dimensional schema (2D) meaning that there is no direct modeling of the hydraulic effect of cross section shape changes, bends, and three-dimensional aspects of flow.

The study allowed us to confirm the validity of the LIDAR technique that allows quickly and easily, updating the geometric characteristics of the waterways.

The models obtained by surveying classic type using interpolation procedures are still very valid in case they are the only ones to which to refer. However, the importance of detail obtained with LIDAR technique allows to define more precisely the trend of tracked river, with the limitations resulting from the difficult-in the presence of high vegetation or submerged parts of the riverbed.

The availability of a DTM with LIDAR technique, corrected by using filtering algorithms more efficient and/or integration with topographic classic, would allow to obtain a procedure for updating automatable in a GIS environment of great utility for the analysis of dangerousness hydraulic territories.

References:

[1] F. Crosilla, D. Visintini, G. Prearo, Filtraggio di dati laser altimetrici con modelli autoregressivi SAR ed algoritmi di ricerca dinamica BFS (BlockForwardSearch),*Atti della 7a Conferenza Nazionale ASITA*, Verona, 2003, pp885-890.

[2] F. Crosilla, D. Visintini, G. Prearo, B. Fico, Esperienze di filtraggio, classificazione, segmentazione e modellazione di dati spaziali da rilievo laser aereo, *Bollettino della SIFET*, Vol.1, 2005, pp. 13-51.

[3] M.A. Brovelli, M. Cannata, U.M. Longoni, Estrazione di DTM da scansione laser: il test comparativo ISPRS, *Atti della VI Conferenza Nazionale ASITA*, Perugia, 2002, pp. 553-558.

[4] V. Casella, Estrazione del DTM di precisione dell'argine di un fiume: fotogrammetria analitica, fotogrammetria digitale e laser scanning a confronto. *Atti della VI*

Conferenza Nazionale ASITA, Perugia, 2001,pp 193-211.

[5] A. Cook, V. Merwade, Effect of topographic data, geometric configuration and modeling approach on flood inundation mapping,*Journal of Hydrology*, Vol.377, 2009, pp. 131-142.

[6] J.R. French, Airborne Lidar in support of geomorphological and hydraulic modelling, *Earth Surface Processes and Landforms*, Vol.28, 2004, pp. 321-335.

[7] M.I. Smith, F.F.F. Asal, G. Priestnall, The use of photogrammetry and lidar for landscape roughness estimation in hydrodynamic studies, *ISPRS*, XXXB part B3, 2004, pp. 714-719.

[8] W.J. Syme, Modelling of bends and hydraulic structures in a two-dimensional scheme, *Conference on Hydraulics in Civil Engineering*, Hobart, 2001.

[9] K. Alphonso, D. Charalampidi, *Generation of DEM from LIDAR data*, 2009.

[10] Autorità di Bacino della Calabria, *Piano Stralcio di Bacino per l'Assetto Idrogeologico (PAI)*, Regione Calabria, 2001.

[11] V. Barrile, D. Lamari, V. Gelsomino, P. Sensini, Modellazione 3d tramite droni per monitoraggi e controlli,*Atti del 61° Convegno nazionale SIFET*, Lecce, 2016.

[12] V. Barrile, G. Bilotta, A. Nunnari, UAV and Computer Vision, Detection of Infrastructure Losses and 3D Modeling, *ISPRS Annals of the Photogrammetry, Remote Sensing and Spatial Information Sciences*, Vol. IV-4/W4, 2017, pp. 135-139.

[13] V. Barrile, V. Gelsomino, D. Lamari, P. Sensini, I Droni e la Computer Vision per la modellazione 3D e individuazione degli ammaloramenti nelle infrastrutture, *Atti della XX Conferenza Nazionale ASITA*, 2016, pp. 690-697.

[14] V. Barrile, V. Gelsomino, G. Bilotta, UAV and Computer Vision in 3D Modeling of Cultural Heritage in Southern Italy. In: International Conference on Materials, Alloys and Experimental Mechanics, IOP Conference Series: Materials Science and Engineering, 2017, Vol. 225.

[15] V. Barrile, G. Bilotta, A. Nunnari, 3D Modeling with Photogrammetry by UAVs and Model Quality Verification, *ISPRS Annals of the Photogrammetry, Remote Sensing and Spatial Information Sciences*, Vol. IV-4/W4, 2017, pp. 129-134.

[16] V. Barrile, G.M. Meduri, G. Bilotta, Laser scanner technology for complex surveying structures,*WSEAS Transactions on Signal* Processing, Vol.7, 2011, pp. 65-74.

[17] V. Barrile, G.M. Meduri, G. Bilotta, Comparison between Two Methods for Monitoring Deformation with Laser Scanner, *WSEAS Transactions on Signal Processing*, Vol.10, 2014, pp. 497-503.

[18] V. Barrile, G.M. Meduri, G. Bilotta, Experimentations and Integrated Applications Laser Scanner/GPS for Automated Surveys, *WSEAS Transactions on Signal Processing*, Vol.10, 2014, pp. 471-480.

[19] US Army Corps of Engineers, *Hydrologic Modeling System, Hec-HMS User's Manual*,2001, http:\\www.usace.army.mil, accessed 26 May 2015.

[20] US Army Corps of Engineers, *Hec-Ras Hydraulic Reference Manual*, 2002,http:\\www.usace.army.mil,accessed 26 May 2015.

[21] P. Mazzoli, L. Perini, L. Cassani, O. Zani, P. Rosetti, LIDAR, strumento topografico per l'aggiornamento dei modelli idraulici, *Estimo e Territorio*, Vol.2, 2007, pp. 27-34.

[22] G. Schumann, P. Matgen, M.E.J. Cutler, A. Black, L. Hoffmann, L. Pfister, Comparison of remotely sensed water stages from LiDAR, topographic contours and SRTM, *ISPRS Journal of Photogrammetry and Remote Sensing*,Vol.63, Issue 3, 2008, pp. 283-296.